Limnol. Oceanogr., 49(3), 2004, 749–755

Optical properties of Asian mineral dust suspended in seawater

Dariusz Stramski[1] *and Sławomir B. Woźniak*[2]
Marine Physical Laboratory, Scripps Institution of Oceanography, University of California at San Diego, La Jolla, California 92093-0238

Piotr J. Flatau
Center for Atmospheric Sciences, Scripps Institution of Oceanography, University of California at San Diego, La Jolla, California 92093-0221; Naval Research Laboratory Monterey, Monterey, California

Abstract

The spectral optical properties of Asian mineral dust suspended in seawater exhibit significant variability associated with the origin (and, hence, the chemistry and mineralogy) and particle size distribution of the samples. The measurements of dust samples from different locations show that the mass-specific absorption coefficient of particles, a_p^*, at a wavelength of light $\lambda = 440$ nm, varies from about 0.028 $m^2\ g^{-1}$ for the soil dust from Chinese desert near Dunhuang to 0.15 $m^2\ g^{-1}$ for the soil dust of volcanic origin in Cheju Island (South Korea). At $\lambda = 400$ nm, this range is 0.05–0.23 $m^2\ g^{-1}$. The aerosol sample collected in the Sea of Japan during a massive dust storm in East Asia shows $a_p^*(\lambda) > 0.1$ $m^2\ g^{-1}$ for $\lambda < 425$ nm. The mass-specific scattering coefficient, $b_p^*(\lambda)$, ranges from about 0.8 to 1.5 $m^2\ g^{-1}$ at blue and green wavelengths for the samples examined. The single scattering albedo, ω_o, increases with wavelength. For $\lambda > 400$ nm, ω_o was >0.78 for the sample from Cheju Island and >0.9 for other samples. In the near-infrared region (750–850 nm), where absorption by dust particles is small or undetectable, ω_o was close to 1.

In the coastal marine environments, mineral particles often represent a significant fraction of suspended particulate matter because of river discharge, coastal erosion by wave and current action, and bottom resuspension. Much of this material is efficiently trapped on the continental shelves and slopes. In the open ocean, it is generally assumed that the abundance of mineral particles is sufficiently low that the optical properties of surface water are dominated by plankton microorganisms and associated detrital matter (Morel and Prieur 1977). However, it has long been recognized that atmospheric transport and the deposition of mineral dust originating from arid and semiarid continental regions covers a large part of the global ocean (Prospero 1990). This source of minerogenic particles has been of major interest to studies of the vertical particle fluxes to the deep ocean (Kremling and Streu 1993) and the delivery of iron to the upper water column (Duce and Tindale 1991). The role of mineral particles in ocean optics remains poorly known, although their potential significance has been suggested even in the oligotrophic ocean (Stramski et al. 2001; Claustre et al. 2002).

The dust storms in China and Mongolia are particularly important as a source of mineral dust over East Asia and North Pacific (Uematsu et al. 1983; Merrill et al. 1989). In the winter, when the land surface is frozen or wet the occurrence of dust storms is low. During the spring, the land warms up and the synoptic disturbances are still strong, which leads to an increase of dust mobilization and aeolian dust transport for long distances. Storm and frontal activity are most prevalent in April, which produces large outflows of complex aerosol mix, including mineral dust and anthropogenic compounds (Merrill et al. 1989; Husar et al. 2001).

The physical, chemical, and radiative properties of Asian aerosol were recently measured from a variety of platforms during the Asia-Pacific Regional Aerosol Characterization Experiment (ACE-Asia), to assess the climate impact of aerosols (Huebert et al. 2003). Unfortunately, the determinations of optical properties of aerosols typically lack direct measurements of the absorption and scattering coefficients over wide spectral range from the near–ultraviolet (near-UV) to near–infrared (near-IR) with high spectral resolution. In addition, the optical properties of aerosols in air are generally not representative of the properties of particles suspended in water. The present article reports on optical determinations for mineral dust samples suspended in seawater. The samples represent dust source regions in China and aerosols collected in the Sea of Japan when a massive dust storm occurred in April 2001 during ACE-Asia.

Materials and Methods

Description of samples—We analyzed four soil dust samples collected in China, one soil dust sample from the Ko-

[1] Corresponding author (stramski@mpl.ucsd.edu).
[2] Current address: Institute of Oceanology, Polish Academy of Sciences, Powstańców Warszawy 55, 81-712 Sopot, Poland.

Acknowledgments

We are grateful to J. Schauer of University of Wisconsin-Madison and P. Chuang of University of California at Santa Cruz for providing soil samples from China and Cheju Island. The analysis of samples for particulate organic carbon was made at Marine Science Institute Analytical Laboratory, University of California at Santa Barbara.

This study was funded by the ONR Environmental Optics Program (grant N00014-98-1-0003 to D.S.), ONR Japan/East Sea DRI (grant N00014-98-1-0247 to B.G. Mitchell and D.S.), the National Science Foundation Climate Dynamics program, and ONR Program Element (PE0602435N to P.J.F.).

Table 1. Identification symbol, type, and origin of the particulate samples from which the aqueous suspension was prepared. The concentration of the dry mass of particles (SPM) in suspension and the concentration of particulate organic carbon (POC) in suspension are given.

Sample ID	Description	Geographical location	SPM ($g\ m^{-3}$)	POC ($g\ m^{-3}$)
URU	Soil, Urumqi, China	43°48′ N, 87°35′ E	17.86	0.785
DUN	Soil, Dunhuang, China	40°30′ N, 94°49′ E	16.13	0.422
ZHE	Soil, Zhenbeitai, China	38°14′ N, 109°48′ E	19.77	0.713
XIA	Soil, Xian, China	34°15′ N, 108°50′ E	18.35	0.660
KOS	Soil, Kosan, Cheju Island	33°29′ N, 126°16′ E	26.14	1.148
JES	Aerosols, Sea of Japan (11–14 Apr 2001)	32°22′ N–37°32′ N 128°36′ E–131°50′ E	17.12	0.963

rean island Cheju, and one aerosol dust sample collected in the Sea of Japan (Table 1, Fig. 1). The samples from China cover a broad range of locations from one of the largest aerosol source regions on Earth. Urumqi (URU) and Dunhuang (DUN) are representative of mineral dust derived from desert areas in northwestern China, the Zhenbeitai (ZHE) sample is from the transitional zone between the desert and the Chinese loess plateau, and Xian (XIA) represents the loess plateau. Cheju is a volcanic island off the southern coast of the Korean peninsula. The soil sample (KOS) from this island was collected at the aerosol sampling station at Kosan. The aerosol sample from the Sea of Japan (referred to as JES for the Japan/East Sea) was collected aboard the NOAA R/V *Ronald H. Brown* during the ACE-Asia cruise. This sample was obtained by dry deposition between 11 and 14 April 2001, when a major dust plume from the Asian continent was transported over the ocean

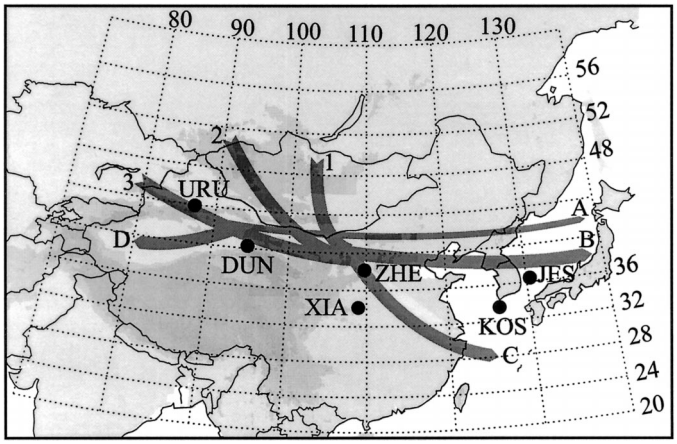

Fig. 1. Location of sampling sites and major atmospheric trajectories of dust transport in East Asia. The north route is indicated as 1, the northwest route as 2, and the west route as 3. The north route is associated with dust storms in the southern Gobi Desert in Mongolia and northern China. Route 2 results in dust storms that occur mainly along the Hexi Corridor and the deserts in northern China. Route 3 causes heavy dust storms in the Hexi Corridor and northern China but also frequently in the Taklimakan Desert. The long range transport routes are indicated as A, B, C, and D (modified after Sun et al. 2001). The sampling stations are: DUN: Dunhuang, JES: Sea of Japan, KOS: Kosan, URU: Urumqi, XIA: Xian, ZHE: Zhenbeitai. Land is shown in shades of gray.

(Gong et al. 2003). The majority of dust deposition during the collection of the JES sample occurred on 11 April 2001. Both the KOS and JES sites are located downwind along the trajectories of prevailing winds that bring dust from the continent.

Optical measurements—Prior to optical measurements, the powder samples of particles were suspended in prefiltered seawater (0.2 μm Nalgene sterile filter, seawater obtained at the pier of the Scripps Institution of Oceanography) and allowed to settle in a small beaker for 30 min to remove large particles from the suspension. The particulate fraction that was still in suspension after the settling period was exposed to ultrasonication for a few minutes. This suspension was then used for optical measurements of the absorption and beam-attenuation coefficients and other analyses.

Measurements of spectral absorption were made with a dual-beam spectrophotometer (Lambda 18; Perkin Elmer) equipped with a 15-cm Spectralon integrating sphere (RSA-PE-18; Labsphere). For each sample, scans of absorbance (or optical density) were made on at least two aliquots of particle suspension in the spectral range from 300 to 850 nm at 1-nm intervals using a 2-nm slit and a scan speed of 120 nm min^{-1}. The replicate scans were averaged to provide the final sample spectrum. The baseline spectrum representing the particle-free reference was measured on seawater filtered through a 0.2-μm filter. Samples and reference were put in 1-cm quartz cuvette in a special holder (Labsphere) at the center of the integrating sphere. This geometry ensures that the absorption measurement of particle suspension is subject to only a small scattering error (Babin and Stramski 2002). However, one problem of this measurement procedure is that small negative values of absorbance are produced in the spectral region where absorption by particles is null or very weak, generally in the near-IR between 700 and 850 nm. This effect has been attributed to differences between the sample and reference measurements in terms of the fraction of incident beam reflected by cuvette walls and then escaping from the integrating sphere through the sample beam port.

A simple way of correcting for this artifact is to shift upward the measured absorbance spectrum by a value corresponding to the negative offset observed in the near-IR region, so the resultant absorption values in that region are zero. We applied such correction to our data, which is re-

ferred to as null-point correction. Because certain types of particles are likely to exhibit some absorption in the near-IR (Tassan and Ferrari 2003), it is important to test the extent of possible violation of the assumption of null-point correction. We estimated an approximate level of near-IR absorption for two samples, DUN and KOS, which exhibited the lowest and highest absorption, respectively, at visible wavelengths among the samples examined. For this purpose, we made additional measurements of these samples with a cuvette tilted by 9° in the holder inside the integrating sphere (Babin and Stramski 2004). The angle of incidence of the primary beam on the cuvette in this modified setup is 9° rather than 0°, as in the normal setup. With the 9° setup, the fraction of the primary unscattered beam, after being reflected on the cuvette wall, does not escape from the integrating sphere through the sample beam port. This eliminates the negative absorbance values observed in the near-IR with the normal setup. Because small scattering/reflection artifacts still existed in the modified setup, it was necessary to determine a position of a ''baseline'' representing the zero absorption in the near-IR. We determined an approximate baseline from measurements on kaolinite suspension (a white powder obtained from Source Clay Minerals Repository, University of Missouri, ref. KGa-1B, which shows negligible absorption in the visible and near-IR; *see* Babin and Stramski 2004). In the baseline determination, the scattering properties of the kaolinite sample were adjusted as close as possible to those of the examined DUN and KOS samples. Specifically, the turbidity of the kaolinite sample (i.e., the beam attenuation coefficient) was adjusted to be nearly identical to that of DUN and KOS, and the particle size distribution of kaolinite sample was also similar to that of DUN and KOS.

The procedure for measuring the spectral beam attenuation coefficient of particles, $c_p(\lambda)$, was similar to that for absorption with the exception of the measurement geometry. For measuring $c_p(\lambda)$, the cuvettes were placed at significant distance from the detector (~25 cm from the entrance port to the integrating sphere), and field stops were aligned within the light path, to reduce the size of the beam and acceptance angle of the detector to <1°. No correction was made for light scattered at very small angles within the receiving aperture of the detector, so the measured $c_p(\lambda)$ may slightly underestimate (by a few percent) the true beam attenuation coefficient (Bricaud et al. 1983). The measurements of $c_p(\lambda)$ were made with a 5-nm slit, which provided a desirable increase in the radiant power of the beam with no adverse effect on the measured $c_p(\lambda)$ spectra, which were relatively smooth and featureless. The optical measurements were made on optically thin suspensions of particles with $c_p < 40$ m^{-1} (<30 m^{-1} for $\lambda > 400$ nm). Thus, for a pathlength of 0.01 m the optical thickness was <0.4. These conditions correspond to the photon mean free path >2.5 cm and negligible effects of multiple scattering within the 1-cm cuvette (Stramski and Piskozub 2003). The beam attenuation measurement was always made first before the absorption measurement, which allowed us to obtain an appropriate optical thickness of the final sample by dilution with particle-free seawater.

The spectral absorption coefficient of particles, $a_p(\lambda)$ in m^{-1}, and the beam attenuation coefficient of particles, $c_p(\lambda)$ in m^{-1}, were calculated by multiplying the baseline-corrected absorbance values of the sample by ln(10) and dividing by the path length (= 0.01 m). The spectral scattering coefficient of particles, $b_p(\lambda)$, was calculated as a difference $c_p(\lambda) - a_p(\lambda)$, and the single scattering albedo of particles, $\omega_o(\lambda)$, as a ratio $b_p(\lambda)/c_p(\lambda)$.

Particle size distribution, dry weight, and particulate organic carbon (POC) analyses—The particle size distribution (PSD) was measured with a Beckman-Coulter Multisizer III equipped with a 30-μm aperture tube using 256 size bins spaced logarithmically between the equivalent spherical diameters (D) of 0.6 and 18 μm. The data for $D < 0.8$ μm are omitted from the analysis, to avoid the effects of instrument noise. In order to minimize coincidence effects (below the 5% level), the particle counts were made on suspensions diluted four times, compared with samples used in the optical measurements. Because the beam attenuation and absorption measurements were separated in time (by no more than 60 min), the size distribution was measured twice—first during the attenuation measurement and then again during the absorption measurement. We observed no significant changes in PSD within the time period necessary to complete the optical measurements. The differences in particle counts were typically <10% for any given size bin in the range of $D < 3$ μm, where particles were most abundant.

In parallel to these measurements, 25–40 ml of sample were filtered onto preweighted 0.2-μm Nuclepore polycarbonate membrane filters (Whatman). These filters were dried at room temperature at relative humidity of 30–40% for 2–3 d before measuring the mass (weight) of particles with a micrometric balance (MT5; Mettler-Toledo). The mass concentration of particles in suspension, referred to as the total suspended particulate matter (SPM), was determined from weight measurements on duplicate filters. The reproducibility between duplicates was within (or better than) 5%. We also tested the 0.02-μm Anopore aluminum oxide membrane filters (Anodisc; Whatman) for particle weight determinations. These tests showed no increase of particle weight compared with that measured on the 0.2-μm filters, which indicates a negligible contribution of particles <0.2 μm in size to the total particulate mass in our samples.

The POC was determined by means of high-temperature combustion with a CEC 440HA Elemental Analyzer (Control Equipment). For these determinations, the samples were prepared by filtering 30–80 ml of the particle suspension onto GF/F filters (Whatman) precombusted at 450°C for 1 h. Before the analysis, the filters were first treated with 0.25 ml of 10% HCl to remove inorganic carbon and then dried at 55°C.

Results and discussion

All samples are dominated by small-sized particles (Fig. 2A,B). The cumulative particle count for the size range 0.8–3 μm varied between 93% and 99% of the total particle count. The concentrations of particles >10 μm were below a detectable level, at least 5 orders of magnitude lower than the concentrations of 1-μm particles. For all samples, the

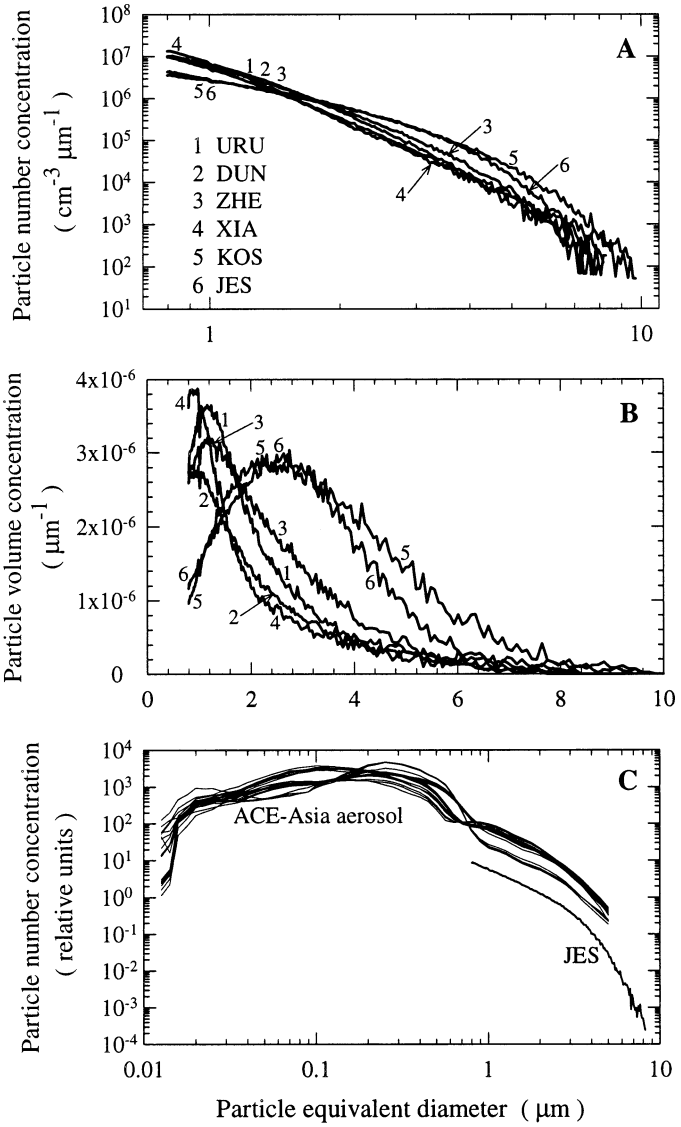

Fig. 2. (A) The density function of particle number size distribution for our samples suspended in seawater as obtained from measurements with a Beckman-Coulter Multisizer III. (B) Same as panel A, but for the particle volume concentration. (C) Comparison of the shape of the particle number size distribution of the JES sample suspended in seawater with the size distributions of aerosol, which were measured on the ACE-Asia cruise during the same day that our JES sample was collected (11 April 2001). The aerosol size distribution data were obtained by a combination of measurements with an ultrafine differential mobility particle sizer (UDMPS) in the range of particles <0.026 μm in size, a differential mobility analyzer (DMPS) in the range of 0.02–0.671 μm, and an aerodynamic particle sizer (APS) in the range >0.54 μm (data from PMEL Atmospheric Chemistry Data Server: http://saga.pmel.noaa.gov/data/index.html).

slope of PSD on a log-log scale became steeper with increasing D. This is consistent with modeling the steady-state particle size distribution in aquatic systems (Burd and Jackson 2002) and measurements of natural seawater samples, which often show a significant change in slope within the diameter range between 1 and 10 μm (Bader 1970; McCave 1975). Compared with a typical slope of -4 (the Junge distribution), our PSDs were somewhat less steep at particle diameters $<$1–1.5 μm and steeper at diameters $>$3–5 μm. The KOS and JES samples showed generally less steep slopes than the remaining samples. The distributions of particle volume concentration of KOS and JES had a maximum between 2 and 3 μm (Fig. 2B). For these samples, about one-half of the total particle volume measured was attributable to particles <3 μm in diameter (46% and 54% for KOS and JES, respectively). For other samples, this percentage was significantly higher (71%–79%). Of interest, the shape of PSD for aqueous suspension of the JES sample was consistent with the shape of size distribution of aerosols measured on the ACE-Asia cruise at the same time that our sample was collected (Fig. 2C).

A small amount of POC relative to SPM (Table 1) indicated that our samples are dominated by mineral particles. If we assume that the dry mass of organic matter was 2.5-fold higher than the POC content (van Raaphorst and Melschaert 1996), an estimate of the contribution of organic matter to SPM varies between 6.5% (DUN) and 14.1% (JES). The mineralogy and chemistry of our samples were not analyzed, but previous studies indicated that aerosols originating from the Asian continent are complex and heterogeneous (Leinen et al. 1994; Gao and Anderson 2001). A global database of the mineral composition of erodible soils shows that the clay fraction of soils from the arid and semiarid regions of China and Mongolia are rich in illite, kaolinite, and smectite and that the silt fraction is dominated by quartz and feldspars with smaller amounts of calcite, iron oxides, and gypsum (Claquin et al. 1999).

The optical spectra of particles discussed below are presented as the mass-specific absorption, $a_p^*(\lambda)$, and scattering, $b_p^*(\lambda)$, coefficients. These coefficients were obtained by normalizing $a_p(\lambda)$ and $b_p(\lambda)$ to the particle mass concentration derived from weight measurements on 0.2 μm Nuclepore filters. All samples exhibited an increase of absorption with decreasing wavelength toward UV, with more or less pronounced changes in the spectral slope in the green, blue, and near-UV regions (Fig. 3A). These spectral features were most likely caused by iron content (Karickhoff and Bailey 1973; Sherman and Waite 1985). Iron can be associated with various mineral species as a structural element in the mineral lattice or exchangeable cation on the particle surface. It can also form crystals of iron oxides and oxide hydroxides such as hematite and goethite. The magnitude of $a_p^*(\lambda)$ exhibits considerable variations among the samples, which was also observed visually as a change in color from pale yellowish (DUN) to dark brown (KOS) for the samples collected on filters. The difference in $a_p^*(\lambda)$ was a factor of >4 at blue wavelengths and a factor of 10 at green wavelengths between the highest values for KOS and the lowest values for DUN. At $\lambda = 440$ nm, a_p^* varied from about 0.028 m^2 g^{-1} for DUN to 0.15 m^2 g^{-1} for KOS. At 400 nm, a_p^* varied from about 0.05 m^2 g^{-1} for DUN to 0.23 m^2 g^{-1} for KOS. This variation is consistent with the range of values observed by Babin and Stramski (2004) for various mineral-dominated particle assemblages, including aerosol-derived Saharan dust and soil particles from the desert areas of northern Africa and Kuwait. The JES sample in our study showed relatively

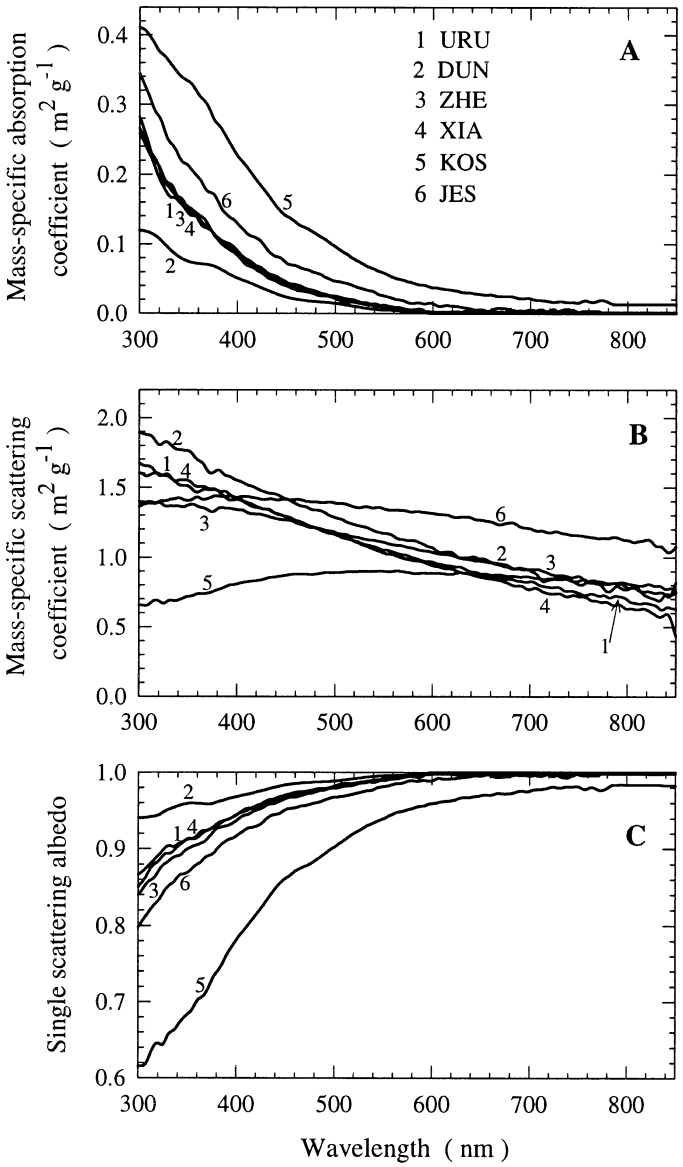

Fig. 3. (A) Spectra of the mass-specific absorption coefficient, (B) mass-specific scattering coefficient, and (C) single-scattering albedo for the samples suspended in seawater. The spectra for DUN and KOS were based on the absorption measurements with a 9° cuvette setup inside the integrating sphere. The spectra for the remaining samples were based on the absorption measurements with a normal cuvette setup inside the sphere and a null correction in the near-IR (see text for details).

strong absorption, with $a_p^*(\lambda) > 0.1$ m^2 g^{-1} for $\lambda < 425$ nm. The URU, ZHE, and XIA samples had nearly identical absorption spectra with intermediate magnitude. Of interest, the most absorbing samples, KOS and JES, were subject to stronger package effect than other samples. The package effect increases with an increase in particle size, which normally results in a reduction of the mass-specific absorption coefficient (Morel and Bricaud 1981). If the particle size distributions of KOS and JES were steeper (like those for other samples; see Fig. 2), the a_p^* values for KOS and JES would be even higher.

The special measurements with a modified measurement system (a 9° cuvette setup) showed that the absorption coefficient of particles in the near-IR can vary from very small or undetectable level (DUN sample) to sizable signal (KOS sample). For DUN, an estimate of the blue ($\lambda = 400$ nm) to near-IR ($\lambda > 700$ nm) absorption ratio was at least 35. The a_p^* values in the near-IR were <0.0015 m^2 g^{-1}. These values were essentially below the level of meaningful detection with our measurement system, because they corresponded to extremely small absorbance values of about 10^{-4}. In contrast, KOS appeared to have sizable absorption in the near-IR. The estimates of the ratio of blue (400 nm) to near-IR (750 and 800 nm) absorption of KOS were ~10 and 17, respectively. The a_p^* values were about 0.015 m^2 g^{-1} at 750 nm and 0.013 m^2 g^{-1} at 800 nm (see curve 5 in Fig. 3A). No special measurements for estimating possible absorption in the near-IR were made for the remaining samples, so they are plotted in Fig. 3A with the zero values in the near-IR. In reality, these samples may exhibit small near-IR absorption in the range between DUN (nearly indistinguishable from zero) and KOS.

The variability in the mass-specific scattering coefficient, $b_p^*(\lambda)$, was smaller than absorption (Fig. 3B). The samples of Chinese soil (URU, DUN, ZHE, and XIA) showed similar $b_p^*(\lambda)$, with the magnitude of scattering increasing considerably toward the short-wavelength portion of the spectrum. XIA showed the steepest wavelength dependence of $b_p^*(\lambda) \sim \lambda^{-1}$ over the spectral region 300–800 nm, with the squared correlation coefficient $r^2 = 0.98$ for the log-transformed variables of λ and b_p^*. For JES, the spectral slope of $b_p^*(\lambda)$ was less steep. The spectral slope was -0.25 over the 300–800 nm region ($r^2 = 0.79$) and -0.37 over the 400–800 nm region ($r^2 = 0.94$). The KOS sample also showed a relatively weak spectral dependence, although, in this case, the scattering increased with λ from the UV to ~560 nm and then decreased with an increase in λ. These differences in the spectral shape between the samples were consistent with the particle size data. The samples having relatively more large particles (KOS and JES) were characterized by weaker dependence of scattering on wavelength. The weaker spectral dependence for KOS and JES can be also partly attributed to an enhanced absorption at short wavelengths, which reduces the scattering in the blue and UV. This effect was especially well-pronounced for KOS.

The observed variability in the wavelength dependence of scattering was generally consistent with the range expected for various particle assemblages in marine environments (Morel 1973; Babin et al. 2003). However, the $b_p^*(\lambda)$ values for our samples were higher than those observed in some coastal waters around Europe by Babin et al. (2003). They reported the typical values of about 0.5 m^2 g^{-1} at 555 nm, which were theoretically explainable by mineral particles that have size distribution with a relatively gentle slope (-4 or less steep) and a low or negligible degree of hydration. Our data for $b_p^*(555)$ ranged from 0.9 for KOS to 1.34 m^2 g^{-1} for JES. For the samples from China, $b_p^*(555)$ was between 1.02 and 1.17 m^2 g^{-1}. The values close to 1 m^2 g^{-1} are considered to be typical for watery organic particles that have a lower density and refractive index than minerals (Babin et al. 2003). Because our samples contained only small

amounts of organic particles, an explanation for the relatively high values of $b_p^*(555)$ may include the rather steep size distribution of mineral particles (with a slope that is effectively steeper than -4), significant hydration of minerals suspended in water, or both. Such characteristics of mineral suspensions in ocean waters would make it difficult, or impossible, to distinguish minerals from organic particles on the basis of the mass-specific scattering coefficient.

The single scattering albedo, $\omega_o(\lambda)$, increased with wavelength and approached 1 in the red and near-IR region (Fig. 3C). By applying our estimates of near-IR absorption (from measurements with the 9° cuvette setup), $\omega_o(\lambda)$ was >0.981 for KOS and >0.998 for DUN at $\lambda > 750$ nm. At visible wavelengths, $\lambda > 400$ nm, $\omega_o(\lambda)$ was >0.78 for KOS and >0.9 for all the remaining samples. The range of ω_o from about 0.8 to 0.9 at 400 nm was consistent with observations from coastal waters and theoretical predictions for mineral particulate assemblages with the Junge-type size distribution (Babin et al. 2003). Because of weak absorption, DUN showed the highest values of $\omega_o(\lambda)$: 0.968 at 400 nm and 0.989 at 500 nm. For JES, $\omega_o(400) = 0.917$, $\omega_o(500) = 0.968$, and $\omega_o(600) = 0.989$.

The knowledge of the optical properties of mineral particles suspended in seawater is a prerequisite to achieving a detailed understanding of the marine optical environment and applying optical techniques in oceanography, including ocean color remote sensing. However, the required quantitative data are still very limited. The prospect for routine determinations of the spectral optical properties of mineral particles from in situ measurements is problematic, because natural assemblages of suspended particles in the ocean are the complex mix of organic and inorganic particles. The theoretical modeling of particle optics has also a limited value because of unavoidable simplifying assumptions about the size, shape, and refractive index of real mineral particles suspended in seawater. Babin and Stramski (2004) reported on laboratory measurements of the absorption properties of various samples dominated by mineral particles, mainly from the arid and semiarid areas in northern Africa. Here we present the absorption and scattering data from laboratory measurements on mineral-dominated particulate assemblages from Asia, which is also a major source region of mineral dust for the Earth's atmosphere and oceans. The laboratory approach allowed us to accurately measure the hyperspectral optical properties of particles, which can additionally be accompanied by analyses of physical and chemical properties of particles.

Although our measurements were not performed on mineral particles isolated from ocean water, we examined a range of natural samples that may be representative of actual mineral assemblages in seawater in terms of mineralogy, size distribution, and associated optical properties. The data from these initial experiments provide quantitative insights into the variability in the spectral optical properties of mineral particles suspended in seawater. This variability underscores a need for more extensive studies, which are additionally called for by potential contribution of mineral particles to ocean optical properties. As an example, this contribution can be assessed by combining our optical data for the JES sample and estimates of deposition rates of Asian dust onto the ocean surface during the dust storm event in April 2001. The dry deposition rate of aerosol particles, F_d, can be calculated as the product of mass concentration of aerosol particles, C_a, in the near-surface atmosphere and a dry deposition velocity, V_d (e.g., Gao et al. 1997). During the dust storm, the concentrations C_a were of $O(10^2)$ μg m^{-3} or higher (Gong et al. 2003). The mean value of dry deposition velocity for polydisperse populations of aerosols over Asian coastal waters can vary from about 1 to 5 cm s^{-1} (Gao et al. 1997). To first approximation, we assumed $C_a = 300$ μg m^{-3} and $V_d = 2$ cm s^{-1}, which yielded $F_d \approx 0.5$ g m^{-2} d^{-1}. The dust episode was observed for several days—at some locations for as long as 2 weeks. Under the tentative assumption that the flux of 0.5 g m^{-2} d^{-1} persisted for 4 d and that the particle concentration after the deposition event was uniform within the mixed layer down to a depth of 30 m (with no particle losses from the mixed layer), we obtained the concentration of mineral dust in surface water of 0.067 g m^{-3}. The product of this concentration and the mass-specific coefficients a_p^* and b_p^* at 440 nm for the JES sample yielded a absorption coefficient, $a_p(440)$, of 0.0055 m^{-1} and a scattering coefficient, $b_p(440)$, of 0.094 m^{-1}. These estimates of potential contribution of mineral particles to the overall absorption and scattering by seawater are significant. The absorption estimate was similar to pure water absorption at 440 nm (0.00635 m^{-1}), and the scattering estimate was nearly 20 times higher than the pure seawater scattering (0.0049 m^{-1}). Although these calculations are simplistic, the results illustrate that the atmospheric deposition of mineral particles can be significant for ocean optical properties, even if we consider the deposition only over a relatively short period of time during a single dust storm event.

References

BABIN, M., A. MOREL, V. FOURNIER-SICRE, F. FELL, AND D. STRAMSKI. 2003. Light scattering properties of marine particles in coastal and open ocean waters as related to the particle mass concentration. Limnol. Oceanogr. **48:** 843–859.

BABIN, M., AND D. STRAMSKI. 2002. Light absorption by aquatic particles in the near-infrared spectral region. Limnol. Oceanogr. **47:** 911–915, 2002.

———, AND ———. 2004. Variations in the mass-specific absorption coefficient of mineral particles suspended in water. Limnol. Oceanogr. **49:** 756–767.

BADER, J. 1970. The hyperbolic distribution of particle sizes. J. Geophys. Res. **75:** 2822–2830.

BRICAUD, A., A. MOREL, AND L. PRIEUR. 1983. Optical efficiency factors of some phytoplankters. Limnol. Oceanogr. **35:** 562–582.

BURD, A. B., AND G. A. JACKSON. 1999. Modeling steady-state particle size distribution. Environ. Sci. Technol. **36:** 323–327.

CLAQUIN, T., M. SCHULZ, AND Y. J. BALKANSKI. 1999. Modeling the mineralogy of atmospheric dust sources. J. Geophys. Res. **104:** 22243–22256.

CLAUSTRE, H., AND OTHERS. 2002. Is desert dust making oligotrophic waters greener? Geophys. Res. Lett. **29:** 10.1029/2001GL014056.

DUCE, R. A., AND N. W. TINDALE. 1991. Atmospheric transport of iron and its deposition in the ocean. Limnol. Oceanogr. **36:** 1715–1726.

GAO, Y., AND J. R. ANDERSON. 2001. Characteristics of Chinese

aerosols determined by individual-particle analysis. J. Geophys. Res. **106:** 18037–18045.

———, AND OTHERS. 1997. Temporal and spatial distributions of dust and its deposition to the China Sea. Tellus **49B:** 172–189.

GONG, S. L., X. Y. ZHANG, T. L. ZHAO, I. G. MCKENDRY, D. A. JAFFE, AND N. M. LU. 2003. Characterization of soil dust aerosol and its transport and distribution during 2001 ACE-Asia. 2. Model simulation and validation. J. Geophys. Res. **108**(D9), 4262, doi: 10.1029/2002JD002633.

HUEBERT, B. J., AND OTHERS. 2003. An overview of ACE-Asia: Strategies for quantifying the relationships between Asian aerosols and their climatic impacts. J. Geophys. Res. **108**(D23), 8633, doi: 10.1029/2003JD003550.

HUSAR, R. B., AND OTHERS. 2001. Asian dust events of April 1998. J. Geophys. Res. **106:** 18317–18330.

KARICKHOFF, S. W., AND G. W. BAILEY. 1973. Optical absorption spectra of clay minerals. Clays Clay Miner. **21:** 59–70.

KREMLING, K., AND P. STREU. 1993. Saharan dust influenced trace element fluxes in deep North Atlantic subtropical waters. Deep-Sea Res. I **40:** 1155–1168.

LEINEN, M., J. M. PROSPERO, E. ARNOLD, AND M. BLANK. 1994. Mineralogy of aeolian dust reaching the North Pacific Ocean. 1. Sampling and analysis. J. Geophys. Res. **99:** 21017–21023.

MCCAVE, I. N. 1975. Vertical flux of particles in the ocean. Deep-Sea Res. **22:** 491–502.

MERRILL, J. T., M. UEMATSU, AND R. BLECK. 1989. Meteorological analysis of long range transport of mineral aerosols over the North Pacific. J. Geophys. Res. **94:** 8584–8598.

MOREL, A. 1973. Diffusion de la lumière par les eaux de mer. Résultats expérimentaux et approche théorique, p. 1–76. *In* Optics of the sea. AGARD Lecture Series, vol. 61, section 3, NATO.

———, AND A. BRICAUD. 1981. Theoretical results concerning light absorption in a discrete medium, and application to specific absorption of phytoplankton. Deep-Sea Res. **28:** 1375–1393.

———, AND L. PRIEUR. 1977. Analysis of variations in ocean color. Limnol. Oceanogr. **22:** 709–722.

PROSPERO, J. M. 1990. Mineral-aerosol transport to the North Atlantic and North Pacific: The impact of African and Asian sources, p. 59–86. *In* A. H. Knap [ed.], The long range atmospheric transport of natural and contaminant substances. Kluwer.

SHERMAN, D. M., AND T. D. WAITE. 1985. Electronic spectra of Fe^{3+} oxides and oxide hydroxides in the near IR to near UV. Am. Mineral. **70:** 1262–1269.

STRAMSKI, D., A. BRICAUD, AND A. MOREL. 2001. Modeling the inherent optical properties of the ocean based on the detailed composition of planktonic community. Appl. Opt. **40:** 2929–2945.

———, AND J. PISKOZUB. 2003. Estimation of scattering error in spectrophotometric measurements of light absorption by aquatic particles from three-dimensional radiative transfer simulations. Appl. Opt. **42:** 3634–3646.

SUN, J., M. ZHANG, M., AND T. LIU. 2001. Spatial and temporal characteristics of dust storms in China and its surrounding regions, 1960–1999: Relations to source area and climate. J. Geophys. Res. **106:** 10325–10333.

TASSAN, S., AND G. M. FERRARI. 2003. Variability of light absorption by aquatic particles in the near-infrared spectral region. Appl. Opt. **42:** 4802–4810.

UEMATSU, M., R. A. DUCE, J. M. PROSPERO, L. CHEN, J. T. MERRILL, AND R. L. MCDONALD. 1983. Transport of mineral aerosol from Asia over the North Pacific Ocean. J. Geophys. Res. **88:** 5343–5352.

VAN RAAPHORST, W., AND J. F. P. MALSCHAERT. 1996. Ammonium adsorption in superficial North Sea sediments. Cont. Shelf Res. **16:** 1415–1435.

Received: 5 August 2003
Accepted: 1 December 2003
Amended: 17 December 2003